Chemical Papers (2020) 74:297–304
https://doi.org/10.1007/s11696-019-00880-0

ORIGINAL PAPER

# Experimental adhesion of *Geobacillus stearothermophilus* and *Anoxybacillus flavithermus* to stainless steel compared with predictions from interaction models

**Jan Strejc[1] · Lucie Kyselova[1] · Anna Cadkova[1] · Dagmar Matoulkova[2] · Tomas Potocar[1] · Tomas Branyik[1]**

Received: 23 April 2019 / Accepted: 12 July 2019 / Published online: 19 July 2019


## Abstract

Spore-forming thermophilic bacteria of the genus *Geobacillus* and *Anoxybacillus* are frequent contaminants in dairy industry. This study is the first attempt to apply models of physicochemical interactions (thermodynamic, DLVO, and XDLVO) to quantify their adhesion properties to stainless steel particles (SSP). The predictions of interaction models were compared with experimental data (contact angles, zeta potentials, size) regarding interacting surfaces (cells and SSP). Adhesion intensities (AI) were determined experimentally taking advantage of the magnetic properties of particulate stainless steel. The importance of weak physicochemical interactions was estimated by comparison of experimental AI with model predictions of colloidal interactions. The results revealed that the most reliable description of AI was obtained using the XDLVO model, including Lifshitz–van der Waals (LW), acid–base, and electrostatic (EL) interactions. The AI of cells to SSP at an ionic strength of 10 mM decreased in the order *G. stearothermophilus* DSM 456 > *A. flavithermus* DSM 2641 > *G. stearothermophilus* DSM 22, and the differences were statistically significant. At a higher ionic strength (100 mM), the highest AI was observed for *A. flavithermus* DSM 2641, but the differences between species studied were statistically insignificant. The main driving force for bacterial adhesion to SSP at 10 mM was EL interactions, while at 100 mM, the XDLVO model predicted favorable interactions between *A. flavithermus* DSM 2641 and SSP due to attractive LW forces.

**Keywords** *Geobacillus* · *Anoxybacillus* · Thermophilic spore formers · Cell adhesion · Stainless steel · Surface interaction models

## Introduction

Representatives of *Geobacillus* and *Anoxybacillus* sp. are Gram positive thermophilic rod-shaped bacteria. Strains of *G. stearothermophilus* are aerobic or facultatively anaerobic while *A. flavithermus* is described as facultatively anaerobic (Nazina et al. 2001; Pikuta et al. 2000; Sadiq et al. 2018). *G. stearothermophilus* contaminates canned products, milk powder, gelatin extracts or cocoa. *A. flavithermus* was isolated from a gelatin extract or milk powder (Burgess et al. 2010; De Clerck et al. 2004; Sadiq et al. 2018). For both *G. stearothermophilus* and *A. flavithermus*, the tendency to spoil dairy products is more likely than canned products (Lücking et al. 2013).

In contrast to thermophilic spores, vegetative cells can be inactivated by heat below 100 °C, although some strains could survive milk pasteurization (Reich et al. 2017). Additionally, biofilm cells can withstand steps like cleaning or sanitization better than planktonic cells (Shi and Zhu 2009).

✉ Tomas Branyik
tomas.branyik@vscht.cz

Jan Strejc
jan_strejc@post.cz

Lucie Kyselova
siristol@vscht.cz

Anna Cadkova
anna.cadkova@gmail.com

Dagmar Matoulkova
matoulkova@beerresearch.cz

Tomas Potocar
potocartom@gmail.com

[1] Department of Biotechnology, University of Chemistry and Technology Prague, Technicka 5, 166 28 Prague, Czech Republic

[2] Department of Microbiology, Research Institute of Brewing and Malting, Lipova 15, 120 44 Prague, Czech Republic

From various possible dairy industry contaminants, the genera *Geobacillus* and *Anoxybacillus* are the most important to treat because of their biofilm-forming potential (Sadiq et al. 2017). Previous studies have shown the potential of *Geobacillus* and *Anoxybacillus* sp. to form biofilms on materials used in dairy industry (Burgess et al. 2014; Cihan et al. 2017; Zhao et al. 2013). Although there are other sources of thermophilic bacilli (TB), like parts of the plant that operate in the optimum thermophile temperature growth range, without biofilm formation the concentrations of TB in milk products would be insignificant (Hill and Smythe 2012).

Adhesiveness to solid surfaces and the biofilm-forming potential of thermophilic dairy spore formers have been studied, where active attachment and biofilm formation of these bacteria on stainless steel has been described (Burgess et al. 2010; Sadiq et al. 2017). It was also found that cell surface properties play a key role in the attachment of TB to processing equipment (Parkar et al. 2001). However, the results are controversial. In one study, a reduced level of hydrophobic stainless steel (SS) surface (dynamic contact angle) attracted more bacterial adhesion (Jindal et al. 2016), while in others, the tendency of cells to adhere to SS decreased with lower cell surface hydrophobicity (adhesion to hydrocarbon) (Jindal and Anand 2018). Agreement was found for cell surface charge, as adhesion of TB to SS decreased with higher cell surface charge (Palmer et al. 2010; Jindal and Anand 2018). Nevertheless, both studies lacked quantitation of SS surface charge (Palmer et al. 2010; Jindal and Anand 2018). Based on the currently available data, it is impossible to quantitatively evaluate the contribution of hydrophobic, electrostatic, or other weak physicochemical interactions to the adhesion of TB to solid surfaces.

The physicochemical aspects of microbial adhesion to solid surfaces can be evaluated using three approaches: (i) the thermodynamic balance of interfacial interactions (Lifshitz–van der Waals and acid–base), used to predict the stability of cell–solid adhesion (van Oss 1995); (ii) DLVO (Derjaguin–Landau–Verwey–Overbeek) theory, estimating the apolar (Lifshitz–van der Waals) and electrostatic interactions; and (iii) extended DLVO (XDLVO) theory, which integrates the two previous approaches (Bos et al. 1999; van Oss 2003). These models have not yet been used to (i) predict adhesion of TB, (ii) compare the prediction with experimental adhesion data and (iii) identify the main driving forces of TB adhesion to solid surfaces.

This work aims to quantify the surface properties of *G. stearothermophilus* (DSM 22, DSM 456) and *A. flavithermus* (DSM 2641) cells and their potential for interaction with SS (AISI 316L). The interaction of thermophilic bacteria with corrosion-resistant stainless steel used in food industry was studied both experimentally and theoretically, using physicochemical models. Experimental adhesion of cells to SS was compared with predictions of thermodynamic and (X)DLVO models in order to identify the main driving forces of cell adhesion.

## Experimental

### Microorganisms and media

The strains used in this study were *G. stearothermophilus* DSM 22 (isolated from deteriorated canned food), *G. stearothermophilus* DSM 456 (isolated from sugar beet juice), and *A. flavithermus* DSM 2641 (isolated from hot spring). Cultivation medium (CM) of the following composition was used (in g/L): casein peptone (5.0, Alfa Aeasar, USA), beef extract (3.0, Sigma Aldrich, Czech Republic), and pH were adjusted to 7. Cultivation was carried out in 500 mL Erlenmeyer flasks (250 mL medium; 150 rpm; 55 °C for *Geobacillus* sp. and 60 °C for *Anoxybacillus* sp.; 24 h for *Geobacillus* sp. and 30 h for *Anoxybacillus* sp.). After cultivation, a cell suspension was obtained by washing twice with distilled water and centrifuging (6000 rpm; 5 min) and immediately used for subsequent tests (image analysis, contact angle, and zeta potential measurements, adhesion tests). The number of spores in cell suspensions at harvesting was less than 6% as observed microscopically (Strejc et al. 2019).

### Contact angles measurement

For the contact angle measurement (CA), a smooth layer of cells was deposited on a membrane filter (47 mm diameter, 0.45 µm pore size, Whatman, USA) under negative pressure using 2.6 mg of dry biomass per $cm^2$ of filter area. The cell lawns were then deposited on agar plates to stabilize their moisture content, fixed on a microscopy glass slide, and allowed to dry for 40 min at 25 °C (Sharma and Hanumantha Rao 2002). Contact angles of stainless steel particles (SSP) (AISI 316L, 60–80 nm, SkySpring Nanomaterials, Inc., TX, USA) were measured in the form of compressed pellets. Pellets were prepared from 1 g of SSP by pressing (7 MPa, evacuable pellet press 13 mm, Pike Technologies, WI, USA). Contact angle measurements were carried out by the sessile drop technique on a CAM 200 goniometer (KSV Instruments, Finland). Drops (volume ≈ 3 µL) of water, formamide, and 1-bromonaphthalene (all from Sigma-Aldrich, Czech Republic) were measured 1 s after placement, ten times for each sample, at 25 °C.

### Zeta potential and cell size measurement

The zeta potentials (ZP) of cells and SSP in contact with electrolyte (10 and 100 mM KCl, pH 7) were measured at 25 °C using a Zetasizer Nano-ZS (Malvern, UK). The cell and nanoparticle suspensions had an absorbance of

0.1 (600 nm). All samples were measured three times with an experimental error ± 10%. The size distribution of SSP was determined microscopically using image analysis software (Bittner et al. 2016). Images of *G. stearothermophilus* (DSM 22, DSM 456) and *A. flavithermus* (DSM 2641) cells were taken using an Olympus BX51 microscope with Olympus C5050 digital camera (min. 100 readings for each strain). For cell size determination, image analysis software (ImageJ, NIH, USA) was used after cell cultivation in CM for 24 h for *Geobacillus* sp. and 30 h for *Anoxybacillus* sp. at 55 and 60 °C, respectively.

## Model calculations

Three physico-chemical interaction models were used to quantify the intensity of interactions between cells and SS particles. The thermodynamic approach was used to calculate the total free energies of interaction from CA values (Table 1) according to van Oss (1995). As representatives of colloidal interactions, the classical DVLO and extended XDLVO theories were used (van Oss 2003). Predictions according to (X)DLVO theories were calculated for model environments (10 and 100 mM KCl, pH 7). For XDLVO the Hamaker constant was estimated from the $\Delta G^{LW}$ values (Table 2)'; the characteristic decay length for acid–base (AB) interactions was 0.6 nm (van Oss 2006), and the intensity of AB interactions was expressed using $\Delta G^{AB}$ values (Table 2).

## Adhesion tests

Quantification of adhesion between cells and SS particles was tested in defined model environments. Cell suspensions (2 mL) of a defined concentration (0.3 ± 0.03 g/L) in electrolyte (10 and 100 mM KCl, pH 7) were mixed (5 rpm, orbital mode, Hulamixer, Invitrogen, USA) with specific amounts of SS particles for 10 min in plastic test tubes. Subsequently, SS particles were exposed to an NdFeB magnet (25 × 10 mm, Neomag, Czech Republic) for 10 min followed by measurement of supernatant absorbance (600 nm). Adhesion intensity (AI, %) was calculated according to the following equation: $AI = [(A_0 - A_1)/A_0] \times 100$, where $A_0$ is the absorbance of the cell suspension and $A_1$ is the absorbance of the supernatant after accelerated magnetic sedimentation. Due to the small size of *Geobacillus* and *Anoxybacillus*, self-sedimentation of cells was negligible. All experiments were performed in triplicate and results are presented as mean values.

Adhesion tests were analyzed by two-way analysis of variance. A post hoc Scheffe's test was used to assess significant differences between the materials. All statements of significance were based on a probability of $p < 0.05$. Statistical analyses were performed using MS Excel software.

**Table 1** Average contact angles and zeta potentials of *Geobacillus stearothermophilus* (DSM 22 and DSM 456), *Anoxybacillus flavithermus* (DSM 2641), and SSP in electrolytes (10 and 100 mM KCl) at pH 7

| Surfaces | Contact angle (°) | | | ZP (mV) | |
|---|---|---|---|---|---|
| | *W* | *F* | *B* | 10 mM | 100 mM |
| DSM 22 | 30.9 ± 1.9 | 54.5 ± 4.0 | 69.3 ± 1.1 | − 24.0 ± 1.1 | − 14.3 ± 1.7 |
| DSM 456 | 35.1 ± 4.5 | 25.9 ± 2.3 | 69.9 ± 2.3 | − 32.9 ± 1.5 | − 15.6 ± 0.9 |
| DSM 2641 | 27.2 ± 1.2 | 58.5 ± 3.8 | 61.0 ± 2.5 | − 23.3 ± 1.0 | − 11.6 ± 1.1 |
| SSP | 25.4 ± 1.1 | 26.9 ± 2.1 | 19.3 ± 2.4 | 17.1 ± 0.8 | − 0.8 ± 1.2 |

*W* water, *F* formamide, *B* 1-bromonaphthalene, *SSP* stainless steel particles

**Table 2** Total surface tensions ($\gamma^{TOT}$) and their apolar ($\gamma^{LW}$) and polar ($\gamma^{AB}$) components and total free energies of interaction ($\Delta G^{TOT}$) and their apolar ($\Delta G^{LW}$) and polar ($\Delta G^{AB}$) components as calculated according to the thermodynamic theory for the system cell–water–cell (cwc) and cell–water–surface (cws) consisting of *Geobacillus stearothermophilus* (DSM 22 and DSM 456), *Anoxybacillus flavithermus* (DSM 2641), and SSP (stainless steel particles)

| Surfaces | Surface tension (mJ/m$^2$) | | | $\Delta G^{TOT}$ (cwc) | $\Delta G^{LW}$ (cws) | $\Delta G^{AB}$ (cws) | $\Delta G^{TOT}$ (cws) |
|---|---|---|---|---|---|---|---|
| | $\gamma^{LW}$ | $\gamma^{AB}$ | $\gamma^{TOT}$ | | | | |
| DSM 22 | 20.3 | 13.1 | 33.4 | 58.2 | 0.6 | 48.7 | 49.3 |
| DSM 456 | 20.0 | 34.8 | 54.8 | 9.6 | 0.7 | 19.2 | 19.9 |
| DSM 2641 | 24.5 | 1.7 | 26.1 | 81.0 | − 1.0 | 57.8 | 56.8 |
| SSP | 41.9 | 8.1 | 50.0 | 31.5 | – | – | – |

## Results

### Physicochemical surface properties of cells and stainless steel particles

Contact angle measurements of the TB studied revealed statistically significant ($p < 0.05$) different CAs of water and formamide for *G. stearothermophilus* DSM 456, and of bromonaphthalene for *A. flavithermus* DSM 2641 (Table 1). The thermodynamic balance of interaction energies based on CA data revealed a broad range of total surface tensions from 26.1 to 54.8 mJ/m$^2$ (Table 2). Calculations of surface tensions revealed prevailing electron donor characteristics ($\gamma^- = 37$–$83$ mJ/m$^2$, $\gamma^+ = 0.01$–$8$ mJ/m$^2$) of all TB studied.

The CA values of TB were also reflected in total free energies of interaction ($\Delta G^{TOT}$) as calculated according to the thermodynamic model for the system cell-water–cell (cwc). Hydrophilic surfaces are characterized by positive $\Delta G^{TOT}$ (van Oss 1995). Given this definition, all TB studied are hydrophilic, although *G. stearothermophilus* DSM 456 was significantly less hydrophilic than the remaining two strains (Table 2).

The CA values of SSP (Table 1) were determined by the compressed pellets method (Bittner et al. 2016) and were used to calculate the appropriate surface tensions (Table 1), which together with positive free energies of interaction ($\Delta G^{TOT}$) of SSP indicate a hydrophilic character of the material (Table 2). Stainless steel particles have a somewhat greater propensity to provide apolar ($\gamma^{LW}$) interactions, as compared to TB (Table 2).

The average ZP values of TB at pH7 in symmetrical model electrolytes (10 and 100 mM KCl) indicate that the cells had a prevailing negative surface charge, which somewhat diminished at higher ionic strengths (IS) (Table 1). The size of SSP in an aqueous environment was determined by Bittner et al. (2016). In colloidal interaction models (DLVO and XDLVO), a diameter of SSP agglomerates of 2 µm was used. The surfaces of SSP could acquire both positive (10 mM) and slightly negative charges (100 mM) independent of the IS (Table 1).

### Prediction of cell–surface interactions and their comparison with adhesion tests

Comparing $\Delta G^{TOT}$ with real adhesion data (Fig. 3), the thermodynamic approach was not able to sufficiently discriminate interaction intensities between TB and SSP. For all combinations of TB with SSP, a negative adhesion energy balance ($\Delta G^{TOT} > 0$) was obtained. This suggests that cell-SSP adhesion would be unfavourable from an energy balance point of view (Table 2), which experimentally was not confirmed, in particular at 10 mM (Fig. 3). Since the thermodynamic model was not able to provide a generalized description of bacterial adhesion to model materials, the classical DLVO and extended DLVO (XDLVO) theories were used.

For (X)DLVO calculations, image analysis was performed to determine the size of vegetative TB cells. Vegetative cells of *G. stearothermophilus* (DSM 22, DSM 456) and *A. flavithermus* (DSM 2641) had the following mean lengths, $4.91 \pm 2.38$, $4.82 \pm 1.73$, and $4.69 \pm 2.88$ µm, and mean diameters, $0.65 \pm 0.35$, $0.50 \pm 0.28$ and $0.82 \pm 0.14$ µm, respectively. In (X)DLVO model predictions, using an approximation of the geometry of a sphere-cylinder, and based on Israelachvili (2011), the mean diameter of rods was chosen as the characteristic size for cells. A simplification neglecting surface roughness of interacting entities was applied in both model predictions.

A simulation of total interaction energies ($G_{DLVO}$) between TB and SSP, as a function of the separation distance at different IS, predicted either the absence or presence of potential energy barriers at the collision of surfaces (Fig. 1). The presence of $G_{DLVO} > 0$ at close contact represents an

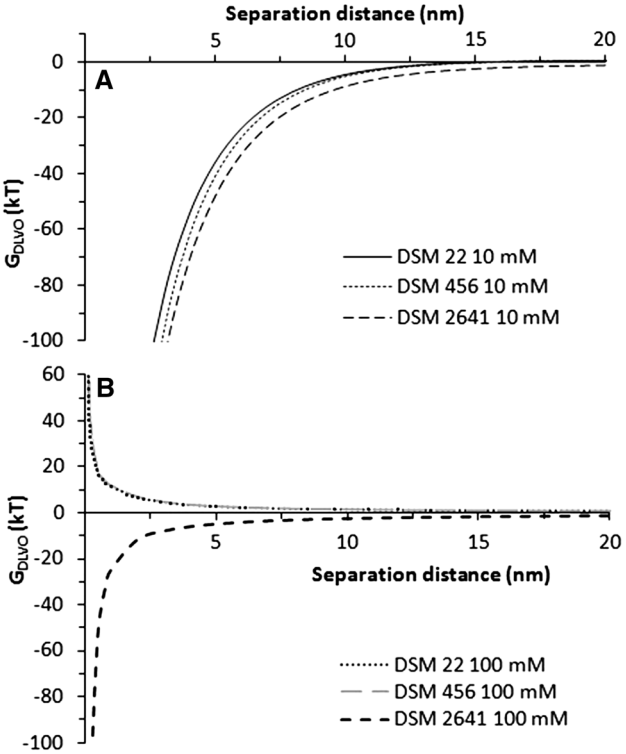


**Fig. 1** Total interaction energy ($G_{DLVO}$) as a function of the separation distance between *Geobacillus stearothermophilus* (DSM 22 and DSM 456), *Anoxybacillus flavithermus* (DSM 2641) and SSP in electrolytes 10 mM KCl (**a**) and 100 mM KCl (**b**) according to the DLVO theory

energy barrier that the approaching surfaces may not overcome. This depends on their kinetic energy. Conversely, a $G_{DLVO} < 0$ predicts an attraction between interacting surfaces. The absence of an energy barrier was predicted for all interactions of TB cells with SSP in 10 mM KCl. For interactions in 100 mM KCl, the absence of energy barriers was predicted for *A. flavithermus* (DSM 2641) vs. SSP, while for *G. stearothermophilus* strains DSM 22 and DSM 456, energy barriers were predicted (Fig. 1). Comparing the DVLO predictions with AI of TB to SSP at an IS of 10 mM (Fig. 3a), it can be seen that the model was unable to qualitatively predict the adhesion of TB to SSP. The $G_{DLVO}$ predictions were very similar, while the AIs were DSM 456 > DSM 2641 > DSM 22 with a statistically significant difference ($p < 0.05$) at the highest SSP-to-cell biomass ratio (Fig. 3a). Similarly, the prediction of no energy barrier at 100 mM for *A. flavithermus* (DSM 2641) does not correspond with the AI, which was higher (statistically not significant) than for the remaining two strains at the highest SSP-to-cell biomass ratio (Fig. 3b).

Although direct contact was unfavorable when there was an energy barrier, the interaction of TB with SSP can take place in a so-called secondary minimum (Redman et al. 2004) (Fig. 2). The depths of secondary minima (SM) predicted by XDLVO were DSM 456 (− 207 kT) > DSM 2641 (− 125 kT) > DSM 22 (− 108 kT) for an IS of 10 mM (Fig. 3a). The main driving forces of TB vs SSP interactions at low IS (10 mM) were the electrostatic interactions (EL), while the acid–base (AB) and Lifshitz–van der Waals (LW) interactions were repulsive, with the exception of LW interactions for *A. flavithermus* DSM 2641. For interactions of TB with SSP at an IS of 100 mM, the XDLVO predicted SM (− 3.2 kT at 7 nm separation distance) only for *A. flavithermus* DSM 2641 (Fig. 2). In this case, the contribution of the LW interaction forces to overall interactions was prevailing and attractive, while the EL and AB interactions were repulsive. Adhesion of TB to SSP increased with increasing MB-to-biomass ratio, often reaching a plateau (Fig. 3). A qualitative agreement was seen between AI (Fig. 3) and the depth of SM, as predicted by the XDLVO model at an IS of 10 mM (Fig. 2). Similarly at an IS of 100 mM, the only SM identified for for *A. flavithermus* DSM 2641 was in accordance with the highest AI observed experimentally (Fig. 3b).

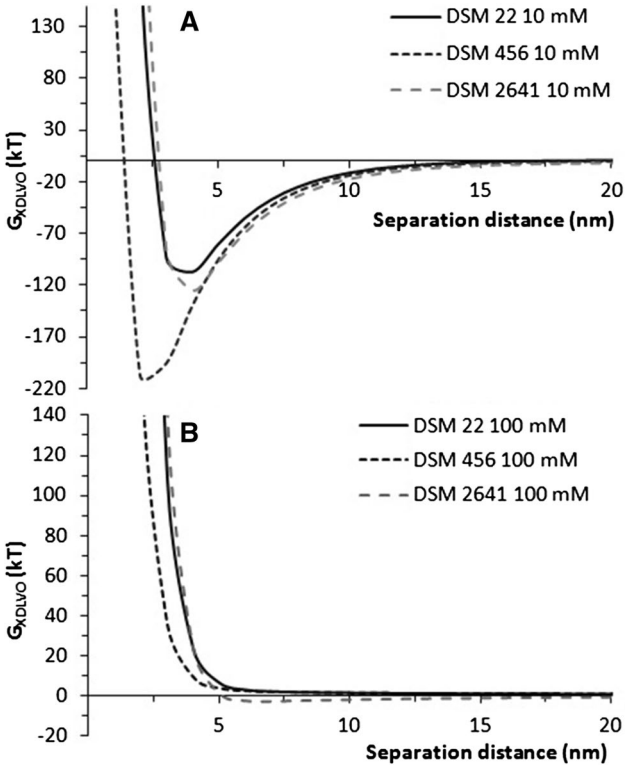


**Fig. 2** Total interaction energy ($G_{XDLVO}$) as a function of the separation distance between *Geobacillus stearothermophilus* (DSM 22 and DSM 456), *Anoxybacillus flavithermus* (DSM 2641), and SSP in electrolytes 10 mM KCl (**a**) and 100 mM KCl (**b**) according to the XDLVO theory

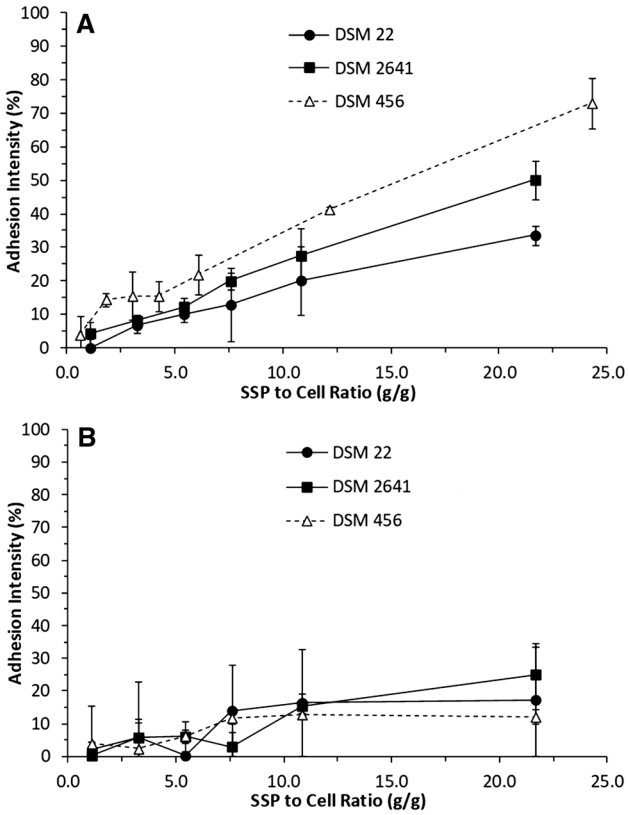


**Fig. 3** Adhesion intensity of *Geobacillus stearothermophilus* (DSM 22 and DSM 456), *Anoxybacillus flavithermus* (DSM 2641) to SSP in 10 mM (**a**) and 100 mM KCl (**b**) at different SSP-to-cell biomass ratios

## Discussion

Spore forming TB are important members of the group of spoilage bacteria in the dairy industry (Burgess et al. 2010). Members of TB contaminate through their presence in multispecies biofilms as a consequence of their ability to adhere to solid surfaces. It can be hypothesized that thermoduric milk spoilers can spread from biofilms either through an aqueous environment and/or by transfer of cells in aerosols (Brandl et al. 2014).

Particulate stainless steel powder was used instead of flat coupons, which are widely applied to study microbial adhesion and/or biofilms (Zhao et al. 2013; Jindal et al. 2016). Although SS is not used widely in the food industry as a particulate material, its advantage lies in its magnetic properties, ease of application, and reproducible character of quantitative adhesion tests (Bittner et al. 2016). In addition, (X)DLVO models take into account the geometry of interacting entities, so predictions are qualitatively valid for any shape of SSP.

In the thermodynamic approach for predicting microbial adhesion to solid surfaces, LW and AB interactions are taken into account. This, however, neglects the role of EL interactions and, therefore, is only valid at close contact (Bos et al. 1999). Yet, the thermodynamic model is capable of quantitatively expressing the contribution of LW and AB forces. Studies available on *Geobacillus* and *Anoxybacillus* species have used microbial adhesion to hydrocarbon (MATH) tests in order to evaluate cell surface hydrophobicity (Palmer et al. 2010; Jindal and Anand 2018). However, no correlation was found between hydrophobicity determined by water CA and MATH tests (Hamadi and Latrache 2008). This paper presents the first surface characterization of these bacterial species by CA measurements and thermodynamic model calculations. The mismatch between thermodynamic interaction energies and experimental AI suggests that electrostatic interactions play a significant role in TB adhesion to SSP. This was also stated in previous studies; however, due to the absence of ZP measurements of (modified) SS coupons, the data were not applicable in colloidal interaction models, and consequently, the EL interactions were not quantifiable (Palmer et al. 2010; Jindal and Anand 2018).

Experimental data on ZP of TB and SSP were obtained and applied in the DLVO model, which integrates short-range LW and long-range EL interactions (Sharp and Dickinson 2005). The comparison between model predictions and adhesion experiments showed that the DLVO model was not able to qualitatively predict the adhesion of TB to SSP. Probably the reason was that the DLVO model neglected AB interactions. Indeed, the XDLVO model, integrating the previous two approaches, showed that AB interactions at separation distances equal to or smaller than the SM, by their repulsive character, equalized and overcame the EL attraction between surfaces. Predictions of XDLVO models were in qualitative agreement with adhesion experiments. More significantly, experimental AI was confirmed by the presence of deeper SM in-model predictions. The consistency between XDLVO model predictions and experimental AI was valid at two IS, varying only at the low IS, where differences between AI of TB were statistically significant ($p < 0.05$). This systematic approach using information on the surface properties of TB and SSP can, therefore, avoid inaccurate conclusions. For instance, an inverse relationship between ZP and bacterial attachment was reported without knowing the ZP of SS coupons at pH 7.4 in phosphate buffer with an unknown IS (Jindal and Anand 2018). The explanation for this observation is that SS at pH 7.4 and IS = 100 mM can have a negative ZP leading to EL repulsion between TB and SSP. However, in an environment with a lower IS at neutral pH (e.g., rinsing water), EL attractions can be stimulated by the positive ZP of SS (Bittner et al. 2016). The importance of EL interactions increases as the IS of the environment decreases. Careful selection of environmental conditions (IS and pH) can, therefore, help to suppress undesirable surface interactions of microorganisms (Sirmerova et al. 2013; Bittner et al. 2017).

In real dairy industry equipment, the formation of biofilms by *A. flavithermus* and *Geobacillus* spp. in milk powder manufacturing lines is mediated predominantly by bacterial physiological factors, e.g., the expression of surface-exposed adhesins (Somerton et al. 2013). Data suggest that both biofilm formation and spore formation of *A. flavithermus* can occur rapidly and simultaneously (Burgess et al. 2009). A previous study demonstrated greater attachment of *G. stearothermophilus* spores to SS coupons compared with vegetative cells (Jindal and Anand 2018). The validity of the XDLVO model for spore attachment should, therefore, be validated in the future.

## Conclusions

In this study, the AI of vegetative cells to SSP was studied in order to quantify the adhesion of TB and demonstrate the prediction potential of colloidal interaction models. Confronting three interaction models with experimental adhesion data resulted in identification of EL interactions as the main driving force for adhesion at low IS, while LW interactions under favourable surface conditions can be attractive even at a higher IS. Consequently, the suppression of unwanted adhesion of TB to SS can be controlled by selecting environmental conditions for cleaning procedures

(IS, pH), the composition of the cleaning agent, and surface treatments of construction materials.

**Acknowledgements** This research was supported by the Ministry of Education, Youth and Sports of the Czech Republic and by the Ministry of Agriculture of the Czech Republic, institutional support MZE-RO1918.

## References

Bittner M, de Souza AC, Brozova M, Matoulkova D, Dias DR, Branyik T (2016) Adhesion of anaerobic beer spoilage bacteria *Megasphaera cerevisiae* and *Pectinatus frisingensis* to stainless steel. LWT Food Sci Technol 70:148–154. https://doi.org/10.1016/j.lwt.2016.02.044

Bittner M, Strejc J, Matoulkova D, Kolska Z, Pustelnikova T, Branyik T (2017) Adhesion of *Megasphaera cerevisiae* onto solid surfaces mimicking materials used in breweries. J Inst Brew 123:204–210. https://doi.org/10.1002/jib.415

Bos R, van der Mei HC, Busscher HJ (1999) Physico-chemistry of initial microbial adhesive interactions—its mechanisms and methods for study. FEMS Microbiol Rev 23:179–230. https://doi.org/10.1111/j.1574-6976.1999.tb00396.x

Brandl H, Fricker-Feer C, Ziegler D, Mandal J, Stephan R, Lehner A (2014) Distribution and identification of culturable airborne microorganisms in a Swiss milk processing facility. J Dairy Sci 97:240–246. https://doi.org/10.3168/jds.2013-7028

Burgess SA, Brooks JD, Rakonjac J, Walker KM, Flint SH (2009) The formation of spores in biofilms of *Anoxybacillus flavithermus*. J Appl Microbiol 107:1012–1018. https://doi.org/10.1111/j.1365-2672.2009.04282.x

Burgess SA, Lindsay D, Flint SH (2010) Thermophilic bacilli and their importance in dairy processing. Int J Food Microbiol 144:215–225. https://doi.org/10.1016/j.ijfoodmicro.2010.09.027

Burgess SA, Flint SH, Lindsay D (2014) Characterization of thermophilic bacilli from a milk powder processing plant. J Appl Microbiol 116:350–359. https://doi.org/10.1111/jam.12366

Cihan AC, Karace B, Ozel BP, Kilic T (2017) Determination of the biofilm production capacities and characteristics of members belonging to *Bacillaceae* family. World J Microbiol Biotechnol 33:118. https://doi.org/10.1007/s11274-017-2271-0

De Clerck E, Vanhoutte T, Hebb T, Geerinck J, Devos J, De Vos P (2004) Isolation, characterization, and identification of bacterial contaminants in semifinal gelatin extracts. Appl Environ Microbiol 70:3664–3672. https://doi.org/10.1128/AEM.70.6.3664-3672.2004

Hamadi F, Latrache H (2008) Comparison of contact angle measurement and microbial adhesion to solvents for assaying electron donor–electron acceptor (acid–base) properties of bacterial surface. Colloid Surf B 65:134–139. https://doi.org/10.1016/j.colsurfb.2008.03.010

Hill BM, Smythe BW (2012) Endospores of thermophilic bacteria in ingredient milk powders and their significance to the manufacture of sterilized milk products: an industrial perspective. Food Rev Int 28:299–312. https://doi.org/10.1080/87559129.2011.635487

Israelachvili JN (2011) Intermolecular and surface forces, 3rd edn. Academic Press, London

Jindal S, Anand S (2018) Comparison of adhesion characteristics of common dairy sporeformers and their spores on unmodified and modified stainless steel contact surfaces. J Dairy Sci 101:5799–5808. https://doi.org/10.3168/jds.2017-14179

Jindal S, Anand S, Huang K, Goddard J, Metzger L, Amamcharla J (2016) Evaluation of modified stainless steel surfaces targeted to reduce biofilm formation by common milk sporeformers. J Dairy Sci 99:9502–9513. https://doi.org/10.3168/jds.2016-11395

Lücking G, Stoeckel M, Atamer Z, Hinrichs J, Ehling-Schulz M (2013) Characterization of aerobic spore-forming bacteria associated with industrial dairy processing environments and product spoilage. Int J Food Microbiol 166:270–279.https://doi.org/10.1016/j.ijfoodmicro.2013.07.004

Nazina TN, Tourova TP, Poltaraus AB, Novikova EV, Grigoryan AA, Ivanova AE, Lysenko AM, Petrunyaka VV, Osipov GA, Belyaev SS, Ivanov MV (2001) Taxonomic study of aerobic thermophilic bacilli: descriptions of *Geobacillus subterraneus* gen. nov., sp. nov. and *Geobacillus uzenensis* sp. nov. from petroleum reservoirs and transfer of *Bacillus stearothermophilus*, *Bacillus thermocatenulatus*, *Bacillus thermoleovorans*, *Bacillus kaustophilus*, *Bacillus thermoglucosidasius* and *Bacillus thermodenitrificans* to *Geobacillus* as the new combinations *G. stearothermophilus*, *G. thermocatenulatus*, *G. thermoleovorans*, *G. kaustophilus*, *G. thermoglucosidasius* and *G. thermodenitrificans*. Int J Syst Evol Microbiol 51:433–446. https://doi.org/10.1099/00207713-51-2-433

Palmer JS, Flint SH, Schmid J, Brooks JD (2010) The role of surface charge and hydrophobicity in the attachment of *Anoxybacillus flavithermus* isolated from milk powder. J Ind Microbiol Biotechnol 37:1111–1119. https://doi.org/10.1007/s10295-010-0758-x

Parkar SG, Flint S, Palmer J, Brooks J (2001) Factors influencing attachment of thermophilic bacilli to stainless steel. J Appl Microbiol 90:901–908. https://doi.org/10.1046/j.1365-2672.2001.01323.x

Pikuta E, Lysenko A, Chuvilskaya N, Mendrock U, Hippe H, Suzina N, Nikitin D, Osipov G, Laurinavichius K (2000) *Anoxybacillus pushchinensis* gen. nov., sp. nov., a novel anaerobic, alkaliphilic, moderately thermophilic bacterium from manure, and description of *Anoxybacillus flavithermus* comb. nov. Int J Syst Evol Microbiol 50:2109–2117. https://doi.org/10.1099/00207713-50-6-2109

Redman JA, Walker SL, Elimelech M (2004) Bacterial adhesion and transport in porous media: role of the secondary energy minimum. Environ Sci Technol 38:1777–1785. https://doi.org/10.1021/es034887l

Reich C, Wenning M, Dettling A, Luma KE, Scherer S, Hinrichs J (2017) Thermal resistance of vegetative thermophilic spore forming bacilli in skim milk isolated from dairy environments. Food Control 82:114–120. https://doi.org/10.1016/j.foodcont.2017.06.032

Sadiq FA, Flint S, Yuan L, Li Y, Liu T, He G (2017) Propensity for biofilm formation by aerobic mesophilic and thermophilic spore forming bacteria isolated from Chinese milk powders. Int J Food Microbiol 262:89–98. https://doi.org/10.1016/j.ijfoodmicro.2017.09.015

Sadiq FA, Flint S, He G (2018) Microbiota of milk powders and the heat resistance and spoilage potential of aerobic spore-forming bacteria. Int Dairy J 85:159–168. https://doi.org/10.1016/j.idairyj.2018.06.003

Sharma PK, Hanumantha Rao K (2002) Analysis of different approaches for evaluation of surface energy of microbial cells by contact angle goniometry. Adv Colloid Interface Sci 98:341–463. https://doi.org/10.1016/S0001-8686(02)00004-0

Sharp FM, Dickinson RB (2005) Direct evaluation of DLVO theory for predicting long-range forces between a yeast cell and a surface. Langmuir 2:8198–8203. https://doi.org/10.1021/la046765s

Shi X, Zhu X (2009) Biofilm formation and food safety in food industries. Trends Food Sci Technol 20:407–413. https://doi.org/10.1016/j.tifs.2009.01.054

Sirmerova M, Prochazkova G, Siristova L, Kolska Z, Branyik T (2013) Adhesion of *Chlorella vulgaris* to solid surfaces, as mediated by physicochemical interactions. J Appl Phycol 25:1687–1695. https://doi.org/10.1007/s10811-013-0015-6

Somerton B, Flint S, Palmer J, Brooks J, Lindsay D (2013) Preconditioning with cations increases the attachment of *Anoxybacillus flavithermus* and *Geobacillus* species to stainless steel. Appl Environ Microbiol 79:4186–4190. https://doi.org/10.1128/AEM.00462-13

Strejc J, Kyselova L, Cadkova A, Potocar T, Branyik T (2019) Physicochemical approach to adhesion of *Alicyclobacillus* cells and spores to model solid materials. Extremophiles 23:219–227. https://doi.org/10.1007/s00792-019-01075-x

van Oss CJ (1995) Hydrophobicity of biosurfaces—origin, quantitative determination and interaction energies. Colloid Surf B 5:91–110. https://doi.org/10.1016/0927-7765(95)01217-7

van Oss CJ (2003) Long-range and short-range mechanisms of hydrophobic attraction and hydrophilic repulsion in specific and aspecific interactions. J Mol Recognit 16:177–190. https://doi.org/10.1002/jmr.618

van Oss CJ (2006) Interfacial forces in aqueous media. CRC Press, Boca Raton

Zhao Y, Caspers MPM, Metselaar KI, de Boer P, Roeselers G, Moezelaar R, Groot MN, Montijn RC, Abee T, Korta R (2013) Abiotic and microbiotic factors controlling biofilm formation by thermophilic sporeformers. Appl Environ Microbiol 79:5652–5660. https://doi.org/10.1128/AEM.00949-13